

# UCLA

## UCLA Previously Published Works

### Title

Pregnancies complicated by gestational diabetes and fetal growth restriction: an analysis of maternal and fetal body composition using magnetic resonance imaging

### Permalink

<https://escholarship.org/uc/item/9zx631zb>

### Journal

Journal of Perinatology, 43(1)

### ISSN

0743-8346

### Authors

Strobel, Katie M  
Kafali, Sevgi Gokce  
Shih, Shu-Fu  
[et al.](#)

### Publication Date

2023

### DOI

10.1038/s41372-022-01549-5

Peer reviewed



Published in final edited form as:

*J Perinatol.* 2023 January ; 43(1): 44–51. doi:10.1038/s41372-022-01549-5.

## Pregnancies Complicated by Gestational Diabetes and Fetal Growth Restriction: An Analysis of Maternal and Fetal Body Composition Using Magnetic Resonance Imaging

Katie M. Strobel, MD MSCR<sup>1</sup>, Sevgi Gokce Kafali, MS<sup>2</sup>, Shu-Fu Shih, MS<sup>2</sup>, Alexandra M. Artura, BS<sup>3</sup>, Rinat Masamed, MD<sup>2</sup>, David Elashoff, PhD<sup>3</sup>, Holden H. Wu, PhD<sup>4</sup>, Kara L. Calkins, MD MSCR<sup>1</sup>

<sup>1</sup>Department of Pediatrics, Division of Neonatology & Developmental Biology, University of California Los Angeles, Los Angeles, CA, USA

<sup>2</sup>Department of Radiological Sciences, University of California Los Angeles, Los Angeles, CA, USA

<sup>3</sup>University of California Los Angeles, Los Angeles, CA, USA

<sup>4</sup>Department of Medicine, Biostatistics and Computational Medicine, University of California Los Angeles, Los Angeles, CA, USA

### Abstract

**INTRODUCTION:** Maternal body composition may influence fetal body composition.

**OBJECTIVE:** The objective of this pilot study was to investigate the relationship between maternal and fetal body composition.

**METHODS:** Three pregnant women cohorts were studied: healthy, gestational diabetes (GDM), and fetal growth restriction (FGR). Maternal body composition (visceral adipose tissue volume (VAT), subcutaneous adipose tissue volume (SAT), pancreatic and hepatic proton-density fat fraction (PDFF) and fetal body composition (abdominal SAT and hepatic PDFF) were measured using MRI between 30 to 36 weeks gestation.

**RESULTS:** Compared to healthy and FGR fetuses, GDM fetuses had greater hepatic PDFF (5.2[4.2,5.5]% vs. 3.2[3,3.3]% vs. 1.9[1.4,3.7]%,  $p=0.004$ ). Fetal hepatic PDFF was associated with maternal SAT ( $r=0.47$ ,  $p=0.02$ ), VAT ( $r=0.62$ ,  $p=0.002$ ), and pancreatic PDFF ( $r=0.54$ ,  $p=0.008$ ). When controlling for maternal SAT, GDM increased fetal hepatic PDFF by 0.9 ([0.51,1.3]%,  $p=0.001$ ).

---

Corresponding Author: Kara L. Calkins MD MSCR, [kcalkins@mednet.ucla.edu](mailto:kcalkins@mednet.ucla.edu).

#### AUTHOR CONTRIBUTIONS:

KMS, HHW, and KLC conceptualized and designed the study. KMS recruited and consented all subjects. KMS, SS, SGK, AA, and RM assisted with data collection and interpretation. KMS performed all the data analysis under guidance of DE. KMS wrote the initial draft of the manuscript. All authors edited and approved the final draft of the manuscript. KLC had the primary responsibility for the final content.

#### ETHICS APPROVAL AND CONSENT TO PARTICIPATE:

The University of California Los Angeles Institutional review board approved the study. Each participant participated with informed consent. The study was performed in accordance with Declaration of Helsinki.

**CONCLUSION:** In this study, maternal SAT, VAT, and GDM status were positively associated with fetal hepatic PDFF.

---

## INTRODUCTION:

Infants born to mothers with gestational diabetes mellitus (GDM) or with a history of fetal growth restriction (FGR) are at increased risk for adult-onset obesity and associated metabolic disorders.<sup>1</sup> The mechanisms contributing to GDM-associated obesity are different from those contributing to FGR-associated obesity. A state of chronic inflammation characterizes GDM and obesity.<sup>2</sup> Adipose tissue releases pro-inflammatory cytokines and free fatty acids that alter the epigenome of the fetus' muscle, liver, and adipose tissue.<sup>2</sup> In contrast, FGR fetuses are exposed to a nutrient-scarce environment.<sup>3</sup> In the FGR fetus, global DNA hypomethylation occurs in the liver along with reduced pancreatic beta cells and lean mass.<sup>3</sup> These adaptations can lead to the future development insulin resistance and type 2 diabetes during childhood and adulthood. Later, GDM and FGR infants exhibit impaired leptin and ghrelin secretion and sensitivity.<sup>4</sup> As a result, they have dysregulated feeding and satiety patterns.

Body composition, the measurement and characterization of lean body mass and adipose tissue, may help explain the different mechanisms and pathophysiological features underlying obesity. Compared to lean mothers, obese mothers are more likely to develop GDM and give birth to macrosomic infants, an independent risk factor for childhood obesity.<sup>5</sup> In adults and children, visceral adipose tissue (VAT) is correlated with pancreatic and hepatic steatosis, biomarkers for insulin resistance and non-alcoholic fatty liver disease (NAFLD).<sup>6,7</sup> On the other hand, in the FGR infant, a lack of fat-free mass has been associated a higher tercile body mass index and poor neurodevelopment.<sup>8</sup>

Body composition can be measured with various technologies. Those involving radiation or air displacement plethysmography are not feasible during pregnancy. Magnetic resonance imaging (MRI) is a noninvasive imaging tool that does not involve ionizing radiation and can be used to accurately quantify the volume of adipose tissue in the infant, child, and adult.<sup>7,9-11</sup> MRI measures the proton-density fat fraction (PDFF, 0-100%), a well-validated biomarker for tissue fat content, and is commonly used to diagnose NAFLD.<sup>12-16</sup> To date, there has been little research on fetal body composition using MRI and no research on body composition during pregnancy. Fetal subcutaneous adipose tissue (SAT) has been identified on MRI in the second and third trimesters.<sup>17,18</sup> In infants, we have used free-breathing 3T MRI to quantify body composition.<sup>11</sup> In pregnant women, we have also utilized free-breathing 3T MRI to characterize placental oxygenation.<sup>19</sup> However, to date, free-breathing MRI has not been used to simultaneously quantify maternal and fetal body composition.

In this pilot prospective cohort study, we aimed to use a motion-compensated free-breathing MRI technique to assess body composition in maternal-fetal dyads in the third trimester of pregnancy. We hypothesized that 1) maternal VAT volume and GDM status would be positively associated with fetal hepatic PDFF and SAT volume, 2) FGR infants would have lower fetal SAT volume than healthy and GDM fetuses, and 3) fetal hepatic PDFF and SAT volume would be positively associated with infant birth growth parameter z-scores.

## MATERIALS/SUBJECTS AND METHODS:

This study was approved by the University of California Los Angeles Institution Medical Review Board. This study was registered at [clinicaltrials.gov](https://clinicaltrials.gov) #20-000599.

### Study Population:

Singleton pregnant women who were less than 36 weeks gestation were eligible for this study. All women provided informed consent before participating in the study. There were three groups: women with healthy pregnancies, women with pregnancies complicated by GDM, and women with pregnancies complicated by FGR. A healthy pregnancy was defined as a pregnancy without fetal anatomic or chromosomal abnormalities, FGR, or GDM. GDM was defined as a positive glucola screen at 26 to 32 weeks gestation.<sup>20</sup> FGR was defined as a fetal weight and abdominal circumference <10<sup>th</sup> percentile on ultrasound for a given gestational age or per obstetrician documentation on at least two medical notes.<sup>21</sup> Exclusion criteria included multiple gestations, fetuses with congenital or chromosomal abnormalities, mothers with prediabetes (hemoglobin A1C  $\geq$  5.5 %) or type II diabetes, and common contraindications to MRI (*e.g.*, claustrophobia, metal implants in the body).

### Study Procedure:

Research MRI exams were performed between 30 to 36 weeks gestation in a non-fasting state. To prevent inferior vena cava compression, women were scanned in the lateral decubitus position. Subjects were given hearing protection. The scan was performed using body and spine array coils on a 3T MRI scanner (MAGNETOM Skyra or Prima, Siemens Healthineers). Sequence parameters are described in Supplementary Table 1. The MRI sequences included in this study were executed under the normal slew rate and specific absorption rate operating mode at 3T. The specific absorption rate for the MRI scanner is regulated by the Food and Drug Administration (FDA).<sup>18</sup> T<sub>2</sub>-weighted (T2W) half-Fourier acquisition single-shot turbo spin-echo (HASTE) scans in coronal, axial, and sagittal orientations were obtained of the fetus for anatomic reference. Free-breathing MRI scans were performed using a prototype 3-D stack-of-radial multi-echo gradient echo Dixon sequence to image the fetal abdomen, fetal neck to the thorax, fetal thorax to the pelvis, and maternal abdomen in the axial orientation.<sup>11,22</sup> If time and the subject permitted, a repeat fetal abdominal scan was performed, and the scan with better image quality was selected for analysis. Twelve subjects had a second abdominal scan. The multi-echo images from the Dixon sequence were used to calculate 3D quantitative PDFF maps (0-100%) based on a seven-peak fat model and a single effective R<sub>2</sub>\* per voxel. For body composition analysis, abdominal MR images and PDFF maps from the 3D axial acquisitions (contiguous slices) were analyzed to measure hepatic PDFF, pancreatic PDFF, SAT volume, and VAT volume. Parameters for MRI sequences are similar to the methods by Armstrong *et al* (see Supplementary information).<sup>11</sup> These MRI sequences followed the FDA guidelines. The overall MRI exam time was approximately 45 to 50 minutes, excluding subject preparation time (approximately 10 minutes).

**Fetal Liver Image Reconstruction:** MR images and PDFF maps were reconstructed and calculated by vendor-provided software on the scanner. In three subjects, the free-

breathing 3-D stack-of-radial MR images and PDFF maps had higher levels of radial streaking artifacts. To improve image quality for these three subjects, we applied an offline reconstruction method that used a phased-array beamforming technique to suppress the artifacts.<sup>23,24</sup>

### Measurement Procedure:

Body composition was measured on MRI by a trained researcher using medical image analysis software (Horos, [thehorosproject.org](http://thehorosproject.org)). All annotated regions of interest were reviewed and verified by an abdominal radiologist with over ten years of experience.

**Fetal Body Composition:** We measured fetal SAT volume and hepatic PDFF. We were unable to visualize and measure VAT volume. Figure 1 shows examples of fetal measurements. Fetal SAT volume was measured on free-breathing 3-D stack-of-radial MRI scans from the level at the mid-liver and the top of the bladder while referring to corresponding sagittal and axial T2W HASTE images for anatomic reference. Volume was calculated by multiplying the area of SAT on a slice by the thickness of the slice. A surrogate of fetal SAT volume was then obtained by calculating the average of the volume from the measurements on the two slices (mid-liver and top of the bladder). Fetal liver PDFF was measured on the free-breathing 3-D stack-of-radial scans.<sup>11</sup> Slices of the liver dome, mid-liver, and inferior liver were compared with the corresponding T2W HASTE axial and sagittal slices to confirm the region of interest (ROI) placement. One 3-cm<sup>2</sup> ROI was placed on each slice while avoiding blood vessels, bile ducts, and regions with increased noise.<sup>11</sup> The liver PDFF was calculated as the mean of these three measurements.

**Maternal Body Composition:** We measured hepatic PDFF, pancreatic PDFF, SAT volume, and VAT volume on free-breathing 3-D stack-of-radial MRI. Figure 2 shows examples of maternal measurements. Maternal liver PDFF was measured by placing one 5-cm<sup>2</sup> ROI on three slices (liver dome, mid-liver, and inferior liver) while avoiding blood vessels, bile ducts, and regions of increased noise.<sup>12–14,25,26</sup> The mean PDFF of these three ROI measurements was calculated. Pancreatic PDFF was measured by outlining the entirety of the pancreas on each slice where it was visible while excluding surrounding vessels, bowel, and fat.<sup>27</sup> The mean PDFF across all slices was calculated. SAT was defined as the adipose tissue above the muscle fascia and below the skin in the abdomen, from the level below breast tissue to below the uterus (approximately 30 slices). VAT was defined as fat around the abdominal organs, from the level of the liver dome to just below the uterus (approximately 30 slices). SAT (or VAT) volume was calculated by multiplying the area of SAT (or VAT) on each slice by the slice thickness and summing across all slices.<sup>7,11</sup>

### Clinical Information Collection:

Maternal information was collected with a focus on risk factors for maternal and childhood obesity and metabolic syndrome (*e.g.* pre-pregnancy body mass index (BMI), weight gain during pregnancy, family history of metabolic diseases, and the etiology of FGR). Information regarding GDM included glucola test results, method of treatment, and percentage of blood glucose concentrations outside of the target range. The following blood glucose concentrations were considered normal: 1. 95 mg/dL if measured in the

pre-prandial state, 2. 140 mg/dL one hour after a meal, or 3. 120 mg/dL two hours after a meal. Infant birth information and growth parameters were collected. The means and standard deviations to calculate z-scores were obtained from Olsen *et al.*<sup>28</sup> Small for gestational age was defined as <10<sup>th</sup> percentile for birth weight using the appropriate growth chart. A research electronic data capture (REDCap) database was used for data management.<sup>29</sup>

### Data Analysis:

All statistical analysis was conducted using JMP Pro version 15.0 (SAS, Carey, NC). Given this was a pilot study, the study was not powered and all results are considered exploratory.

**Cohort Characteristics:** Frequency (%) was used for descriptive variables. Variables were compared between cohorts using Fischer's exact tests. Continuous variables were described with medians and interquartile ranges. Continuous variables were compared between cohorts using Kruskal-Wallis tests with Dunn's tests for two-sided pairwise comparisons. Variance was similar between cohorts. Given sample size, pairwise comparisons were not adjusted.

**Body Composition Comparisons:** All body comparisons utilized all the women involved in the study. Fetal body composition measurements were correlated to maternal pre-pregnancy BMI, maternal weight gain during pregnancy, gestational age at the time of MRI, infant birth z-scores, maternal SAT volume, maternal VAT volume, maternal pancreatic PDFF, and maternal liver PDFF using linear regression models and Spearman correlation coefficients. Maternal body composition measurements were correlated with maternal pre-pregnancy BMI, maternal weight gain during pregnancy, gestational age at the time of MRI, and fetal body composition measurements using linear regression models and Spearman correlation coefficients. To further investigate associations with fetal hepatic PDFF, a multivariable linear regression model was conducted using stepwise backward variable selection to minimize BIC. Candidate variables were selected based on biological relevance and significant correlations. The following candidate variables were selected: gestational age at MRI, pre-pregnancy BMI, maternal SAT volume, VAT volume, and pancreatic PDFF and GDM status (yes/no).

## RESULTS:

### Cohort Characteristics:

From September 2020 to July 2021, pregnant women were recruited to participate in the study. 20 maternal-fetal dyads completed the study (Supplementary Figure 1). Maternal, fetal, and infant characteristics are described in Table 1. All GDM women had a positive 1- and 3-hour glucola tolerance test. Four GDM women required insulin; one mother's GDM was diet-controlled. At the first endocrinology visit, 19 (6, 23) % of the glucose concentrations on the glucose log were out of goal range. At the second endocrinology visit, 25 (13,26) % of the glucose concentrations on the glucose log were out of goal range. The etiology in four FGR cases was uteroplacental insufficiency; the etiology in one FGR

case was poor maternal nutrition. Fetuses with FGR were more likely to be admitted to the neonatal intensive care unit compared to infants in the healthy and GDM cohorts ( $p=0.04$ ).

Cohort body composition parameters are described in Table 2. Mothers with GDM had greater VAT volume than mothers with healthy pregnancies ( $p=0.04$ ) and a higher pancreatic PDFF compared to the mothers in the FGR cohort ( $p=0.03$ ). Fetuses of GDM mothers had greater SAT volume ( $p=0.002$ ) and hepatic PDFF ( $p=0.008$ ) than growth restricted fetuses. Fetuses of GDM mothers had greater hepatic PDFF than fetuses of healthy mothers ( $p=0.002$ ) and greater SAT volume than healthy mothers but this was not statistically different ( $p=0.10$ ).

### Fetal Body Composition and Maternal Characteristics:

Fetal SAT volume positively correlated with gestational age at the time of the MRI ( $r=0.45$ ,  $p=0.03$ ) with an increase of 8.6 (95% CI 1.2, 16)  $\text{mm}^3$  per week during gestation. All other maternal and fetal body composition parameters did not correlate with gestational age (all  $p$ -values  $>0.05$ ).

Maternal pre-pregnancy BMI was positively associated with maternal SAT volume (12161 [95% CI 5413, 18909]  $\text{mm}^3/\text{kg}/\text{m}^2$ ;  $r=0.64$ ,  $p=0.001$ ), maternal pancreatic PDFF (0.27 [95% CI 0.092, 0.45]  $\%/ \text{kg}/\text{m}^2$ ;  $r=0.57$ ,  $p=0.005$ ), maternal VAT volume (8466 [95% CI 5937, 10995]  $\text{mm}^3/\text{kg}/\text{m}^2$ ;  $r=0.85$ ,  $p<0.001$ ), and fetal hepatic PDFF (0.11 [95% CI 0.032, 0.21]  $\%/ \text{kg}/\text{m}^2$ ;  $r^2=0.53$ ,  $p=0.01$ ). Maternal weight gain in pregnancy was negatively associated with maternal VAT volume ( $-7393$  [95% CI  $-12889$ ,  $-1896$ ]  $\text{mm}^3/\text{kg}$ ;  $r=0.54$ ,  $p=0.01$ ) and maternal pancreatic PDFF ( $-0.41$  [95% CI  $-0.62$ ,  $-0.20$ ]  $\%/ \text{kg}$ ;  $r=0.69$ ,  $p=0.001$ ). Maternal weight gain in pregnancy was not associated with other maternal or fetal body composition parameters ( $p>0.05$  for all). Maternal serum glucose levels one hour after a glucola challenge were positively associated with maternal pancreatic PDFF (0.025 [95% CI 0.0028, 0.047]  $\%/ \text{mg}/\text{dL}$ ;  $r^2=0.21$ ,  $p=0.03$ ), fetal SAT volume (0.42 [95% CI 0.15, 0.69]  $\text{mm}^3/\text{mg}/\text{dL}$ ;  $r^2=0.35$ ,  $p=0.01$ ), and fetal liver PDFF (0.013 [95% CI 0.001, 0.026]  $\%/ \text{mg}/\text{dL}$ ;  $r^2=0.18$ ,  $p=0.04$ ).

Fetal SAT volume was positively associated with maternal pancreatic PDFF (5.1 [95% CI 0.30, 9.8]  $\text{mm}^3/\%$ ;  $r=0.42$ ,  $p=0.04$ ). Fetal SAT volume was not associated with maternal hepatic PDFF, maternal SAT volume, or maternal VAT volume ( $p>0.05$  for all). Fetal hepatic PDFF was positively associated with maternal pancreatic PDFF (0.27 [95% CI 0.77, 0.46]  $\%/ \%$ ;  $r=0.54$ ,  $p=0.008$ ), SAT volume ( $5.9 \times 10^{-6}$  [95% CI  $9.5 \times 10^{-7}$ ,  $1.1 \times 10^{-5}$ ]  $\%/ \text{mm}^3$ ;  $r=0.47$ ,  $p=0.02$ ), and VAT volume ( $1.39 \times 10^{-5}$  [95% CI  $5.8 \times 10^{-6}$ ,  $2.2 \times 10^{-5}$ ]  $\%/ \text{mm}^3$ ;  $r=0.62$ ,  $p=0.002$ ) (Figure 3).

When conducting a multivariable linear regression model, maternal SAT volume and GDM status were selected with an  $r=0.81$ , Bayesian information criterion 50. When controlling for maternal SAT volume, GDM status increased fetal liver PDFF by 0.9 [95% CI 0.51, 1.3],  $p=0.001$ . When controlling for GDM status, maternal SAT volume positively increased fetal hepatic PDFF by 0.0393%/10,000  $\text{mm}^3$  [95% CI 0.0049%/10,000  $\text{mm}^3$ , 0.073%/10,000  $\text{mm}^3$ ],  $p=0.03$ .



### Maternal and Fetal Body Composition and Infant Growth:

Fetal SAT volume was positively associated with infant birth weight z-score, increasing by 0.02 (95% CI 0.011,0.033) z-score units per 1 mm<sup>3</sup> of SAT volume ( $r=0.72$ ,  $p<0.001$ ). Maternal body composition was not associated with any infant growth parameters.

### DISCUSSION:

In this pilot study, we used free-breathing MRI to examine the relationship between maternal adiposity and fetal body composition in uncomplicated pregnancies, pregnancies with GDM, and pregnancies complicated by FGR. Consistent with other studies, fetal SAT volume increased with gestational age<sup>30,31</sup> and was associated with birth weight z-score.<sup>32,33</sup> Maternal pre-pregnancy BMI was positively correlated with maternal pancreatic PDFF, maternal SAT volume, maternal VAT volume, and fetal hepatic PDFF. Consistent with obstetrician recommendations of limited weight gain in the setting of obesity, maternal weight gain in pregnancy was negatively associated with maternal VAT volume and pancreatic PDFF.<sup>34</sup> Maternal pancreatic PDFF, SAT volume, and VAT volume positively correlated with fetal hepatic PDFF. Our multivariable regression model suggested that GDM and maternal SAT volume were significant contributors to fetal hepatic PDFF compared to VAT volume and pre-pregnancy BMI.

In our study, the GDM cohort had a greater amount of fetal hepatic PDFF compared to the healthy cohort and FGR cohort and greater SAT volume than the FGR cohort. Previous literature has shown a greater SAT volume in fetuses whose mothers have GDM compared to fetuses of healthy women with a normal BMI.<sup>32</sup> In our study, there was no statistically significant difference in fetal SAT volume between the GDM group and healthy group, but there was a trend toward a greater fetal SAT volume in the GDM cohort compared to the healthy cohort. This negative finding may be because of our small sample size. Moreover, two of the healthy subjects had a pre-pregnancy BMI  $>25$  kg/m<sup>2</sup>; one subject was overweight; the other subject was obese. As a result, we are unable to accurately disentangle the effects of maternal obesity and GDM on fetal body composition.

Several mechanisms may explain why GDM fetuses have increased SAT volume and altered body composition as a fetus and infant.<sup>32</sup> First, pregnancies complicated by GDM are hallmarked by an increase in placental glucose, amino acid, and fatty acid transport, which increases the fetus's endogenous production of insulin and insulin-like growth factor 1.<sup>35</sup> Insulin-like growth factor-1 has been associated with an increase in SAT in mice.<sup>36</sup> Second, the metabolite profile in amniotic fluid is altered in fetuses born to mothers with GDM. N1-methyl-4-pyridone-3-carboxamide, 5'-methylthioadenosine, and kynurenic acid are associated with GDM severity and fetal growth.<sup>37</sup> These metabolites alter steroid hormones and carbohydrate metabolism. Last, leptin and adiponectin, two hormones involved in energy metabolism and insulin regulation, are increased in infants born to mothers with GDM. One study found that infants of diabetic mothers at delivery had increased umbilical cord blood leptin and adiponectin concentrations.<sup>38</sup> Umbilical cord blood leptin was positively associated with SAT.<sup>39</sup>



In this study, FGR fetuses had decreased hepatic PDFF and SAT volume compared to GDM fetuses. In ultrasound studies of FGR fetuses and infants, decreased abdominal SAT was associated with a lower infant triceps and subscapular skinfold thickness and infant abdominal circumference.<sup>39</sup> The FGR cohort likely had less SAT due to a nutrient-deprived state in-utero. In this study, four women had placental insufficiency, and one woman had insufficient caloric intake. In this nutrient-limited environment, fetuses with growth restriction have decreased lean body mass. Research has found that decreased lean body mass persists into adulthood for those with FGR. Decreased muscle mass with superimposed “catch up” growth (increased fat mass) in childhood may increase the risk for future metabolic diseases.<sup>40</sup> Studies have found that increased weight gain and BMI in small for gestational age infants led to higher fat mass as a toddler<sup>41</sup> and insulin resistance at six years of age.<sup>42</sup> These findings are consistent with the theory that an early adiposity rebound is associated with childhood obesity.<sup>43</sup> Unfortunately, we were unable to assess lean body mass in this study.

Although previous research regarding fetal body composition has focused on SAT, our study also assessed fetal hepatic and maternal pancreatic PDFF. Fetal hepatic PDFF was positively correlated with maternal adiposity and GDM status. To date, there is no literature examining human fetal hepatic fat. In a study of pregnant guinea pigs, maternal and fetal hepatic fat content measured by MRI was greater in the animals exposed to a Western diet than animals exposed to a standard diet.<sup>44</sup> In a murine study, fetal livers of pregnant mice fed a high-fat diet and who developed NAFLD were compared fetal livers of pregnant mice who were fed a standard diet. Fetal liver inflammation, apoptosis, steatosis, and oxidative stress were notably increased in mice whose mothers had NAFLD compared to the control group.<sup>45,46</sup> These fetal liver changes were associated with impaired glucose tolerance and decreased insulin sensitivity at postnatal day 15.<sup>47</sup> Fetal hepatic fat may play an important role in future metabolic health.<sup>48</sup> Future longitudinal studies are needed to understand the relationship between GDM and maternal obesity and the offspring’s risk for NAFLD.

In our study, increased maternal pancreatic PDFF, SAT volume, and VAT volume was associated with increased fetal liver PDFF. In previous ultrasound studies, maternal VAT depth in the second trimester was associated with an increase in birth weight.<sup>49,50</sup> There have been no studies to date that have examined the relationship between maternal pancreatic fat and the offspring’s body composition. One animal study found that increased maternal VAT in mice on a high fat diet was associated with impaired pancreatic function in pregnant mice.<sup>51</sup> We suspect maternal adiposity alters fetal body composition and infant growth through epigenetic changes involving adiponectin. Compared to the SAT of lean women, the SAT of obese women is characterized by an increase in the methylation of the adiponectin gene and decrease in adiponectin mRNA.<sup>52</sup> Women with increased adiposity have less adiponectin, which has an inverse relationship with FGR.<sup>53</sup> Low circulating adiponectin in obese mothers does not limit insulin’s effect, leading to aberrant placental nutrient transfer and excessive fetal growth.<sup>53</sup>

In this study, a pregnancy complicated by GDM was associated with an increase in fetal SAT volume and hepatic PDFF. GDM was the primary driver of fetal hepatic PDFF in the multi-variable linear regression model despite a small sample size. In a study of infants

born to mothers with GDM, these infants had increased fat-mass and skinfold thickness, and maternal serum glucose concentrations had the strongest relationship with infant adiposity.<sup>54</sup> One study examining infants born to obese mothers using 1.5T MR spectroscopy found that infants of obese mothers with GDM had increased hepatic fat compared to infants of healthy mothers without GDM.<sup>55</sup> Another study examined fetal SAT volume utilizing MRI found at 34 weeks gestation. In this study, the overweight and GDM cohort had increased fetal SAT volume compared to controls.<sup>32</sup> In our study, all of the women in the GDM cohort were overweight or obese, and almost all women required medications to manage their GDM. In a mouse study, hepatic steatosis was noted in fetuses of pregnant mice exposed to a Western diet compared to a fetuses of pregnant mice fed a standard diet.<sup>44</sup> However, when the pregnant mice exposed to a Western diet were given metformin early in pregnancy, the amount of fetal hepatic fat between the two groups was comparable.<sup>45</sup> In an MRI study examining fetal SAT volume in women without and with GDM and with a BMI <30 kg/m<sup>2</sup> and >30 kg/m<sup>2</sup>, fetal SAT volume was similar among women with a BMI <30 kg/m<sup>2</sup> regardless of GDM.<sup>30</sup> These findings emphasize the need for future research to examine the complex relationship between adiposity and GDM.

We recognize our study's limitations. MRI machines are costly, loud, not easily accessible, and require subjects to be in an enclosed space. A common problem with MRI is motion artifacts. To mitigate the impact of fetal motion, we avoided placing ROIs in motion affected areas, and all measurements were performed by a trained research fellow and confirmed by an abdominal radiologist. Attempts to optimize fetal MRI sequences with a phantom scan (i.e., reference object) are technically difficult due to the inability to simulate fetal motion.<sup>56</sup> 3-D stack-of-radial sampling sequences help mitigate motion artifacts in adults, children, and infants and may be of use for fetal MRIs.<sup>26,25,11</sup>

We are unable to validate our measurements for two main reasons. First, it is not ethical to perform a fetal biopsy for validation of MRI fetal body composition measurements. Second, while hepatic PDFF has been validated with biopsy in adults, it has not been validated in the fetus.<sup>57</sup> However, fetal SAT volume has been consistently identified in the third trimester of pregnancy.<sup>17,18,30-32</sup> Giza *et al.* utilized a similar method of sequencing and fat segmentation, and our results are consistent with this study.<sup>31</sup> In the future, we plan to evaluate intra- and inter-observer variability of our fetal measurements.

Because this is a pilot study, our sample size is limited, and the results should be considered exploratory. Gestational age is known to influence specific body composition measurements.<sup>30,31</sup> However, gestational age was not included in the multi-variable model because of the study's small sample size. Lastly, we did not longitudinally measure body composition during pregnancy and infancy. Future follow-up would be required to understand if maternal and fetal body composition are truly associated with future childhood and adulthood obesity and various metabolic complications.

In conclusion, to our knowledge, this is the first study to quantify maternal body composition and fetal hepatic PDFF at the same time using free-breathing MRI technology. Fetal SAT volume was positively associated with infant birth weight z-score. Fetuses exposed to GDM had a greater amount of fetal SAT volume compared to growth restricted

fetuses. Moreover, fetuses exposed to GDM had a greater amount of hepatic PDFF compared to fetuses with growth restriction and fetuses of healthy mothers. Maternal pre-pregnancy BMI, pancreatic PDFF, VAT volume, and SAT volume were positively correlated with fetal hepatic PDFF. We speculate that maternal adiposity and insulin resistance increase fetal hepatic fat content and the offspring's risk for future obesity and NAFLD.

## Supplementary Material

Refer to Web version on PubMed Central for supplementary material.

## ACKNOWLEDGMENTS:

The authors would like to acknowledge Dr. Carla Janzen, Dr. Michelle Tsai, Dr. Alexandra Havard, Dr. Ilina Pluym, and Dr. Thalia Wong who assisted with recruitment and provided insight into maternal data. The authors would also like to thank the MRI technologists at University of California Los Angeles for assisting with the study.

## FUNDING:

KMS received research support from University of California Los Angeles Children's Discovery Institute. HHW and KLC received funding from NIH/NIDDK R01-124417-01.

## COMPETING INTERESTS:

KLC has received research support from Fresenius Kabi. KLC has served as an advisor for Fresenius Kabi, Mead Johnson, Baxter, and Prolacta. KLC serves as an institutional principal investigator, with no salary funding, for a consortium database sponsored by Mead Johnson. HHW receives research support from Siemens Medical Solutions USA.

## DATA AVAILABILITY:

The data that supports the findings of this study are available from the corresponding author upon reasonable request and may require institutional data agreements.

## Abbreviations:

<b>GDM</b>	Gestational diabetes
<b>FGR</b>	Fetal growth restriction
<b>CT</b>	Computerized tomography
<b>MRI</b>	Magnetic resonance imaging
<b>PDFF</b>	Proton density fat fraction
<b>SAT</b>	Subcutaneous adipose tissue
<b>NAFLD</b>	Non-alcoholic fatty liver disease
<b>ROI</b>	Region of interest
<b>VAT</b>	Visceral Adipose Tissue
<b>BMI</b>	Body mass index

## REFERENCES/BIBLIOGRAPHY:

1. Ornoy A Prenatal origin of obesity and their complications: Gestational diabetes, maternal overweight and the paradoxical effects of fetal growth restriction and macrosomia. *Reprod Toxicol.* 2011 Sep;32(2):205–12. doi: 10.1016/j.reprotox.2011.05.002. Epub 2011 May 19. [PubMed: 21620955]
2. Johns EC, Denison FC, Norman JE, Reynolds RM. Gestational Diabetes Mellitus: Mechanisms, Treatment, and Complications. *Trends Endocrinol Metab.* 2018 Nov;29(11):743–754. doi: 10.1016/j.tem.2018.09.004. Epub 2018 Oct 5. [PubMed: 30297319]
3. Thorn SR, Rozance PJ, Brown LD, Hay WW. The Intrauterine Growth Restriction Phenotype: Fetal Adaptations and Potential Implications for Later Life Insulin Resistance and Diabetes. *Semin Reprod Med.* 2011 29 (3): 225–236. [PubMed: 21710398]
4. Ross MG, Desai M. Developmental programming of offspring obesity, adipogenesis, and appetite. *Clin Obstet Gynecol.* 2013;56(3):529–536. doi:10.1097/GRF.0b013e318299c39d [PubMed: 23751877]
5. Kc K, Shakya S, Zhang H. Gestational diabetes mellitus and macrosomia: a literature review. *Ann Nutr Metab.* 2015;66 Suppl 2:14–20. doi: 10.1159/000371628. Epub 2015 Jun 2.
6. Wang Y, He S, He J, Wang S, Liu K, Chen X. Predictive value of visceral adiposity index for type 2 diabetes mellitus: A 15-year prospective cohort study. *Herz.* 2015 May;40 Suppl 3:277–81. doi: 10.1007/s00059-014-4175-1. Epub 2014 Nov 21. [PubMed: 25410470]
7. Ly KV, Armstrong T, Yeh J, Ghahremani S, Kim GH, Wu HH, et al. Free-breathing Magnetic Resonance Imaging Assessment of Body Composition in Healthy and Overweight Children: An Observational Study. *J Pediatr Gastroenterol Nutr.* 2019 Jun;68(6):782–787. doi: 10.1097/MPG.0000000000002309. [PubMed: 30789865]
8. Frondas-Chauty A, Simon L, Flamant C, Hanf M, Darmaun D, Rozé JC. Deficit of Fat Free Mass in Very Preterm Infants at Discharge is Associated with Neurological Impairment at Age 2 Years. *J Pediatr.* 2018 May;196:301–304. doi: 10.1016/j.jpeds.2017.12.017. Epub 2018 Jan 11. [PubMed: 29336797]
9. Borga M, West J, Bell JD, Harvey NC, Romu T, Heymsfield SB, et al. Advanced body composition assessment: from body mass index to body composition profiling. *J Investig Med.* 2018 Jun;66(5):1–9. doi: 10.1136/jim-2018-000722. Epub 2018 Mar 25.
10. Ross R Magnetic resonance imaging provides new insights into the characterization of adipose and lean tissue distribution. *Can J Physiol Pharmacol.* 1996 Jun;74(6):778–85. [PubMed: 8909791]
11. Armstrong T, Ly KV, Ghahremani S, Calkins KL, Wu HH. Free-breathing 3-D quantification of infant body composition and hepatic fat using a stack-of-radial magnetic resonance imaging technique. *Pediatr Radiol.* 2019 Jun;49(7):876–888. doi: 10.1007/s00247-019-04384-7. Epub 2019 Apr 17. [PubMed: 31001664]
12. Reeder SB, Hu HH, Sirlin CB. Proton density fat-fraction: a standardized MR-based biomarker of tissue fat concentration. *J Magn Reson Imaging.* 2012 Nov;36(5):1011–4. doi: 10.1002/jmri.23741. Epub 2012 Jul 6. [PubMed: 22777847]
13. Yokoo T, Serai SD, Pirasteh A, Bashir MR, Hamilton G, Hernando D, et al. RSNA-QIBA PDFF Biomarker Committee. Linearity, Bias, and Precision of Hepatic Proton Density Fat Fraction Measurements by Using MR Imaging: A Meta-Analysis. *Radiology.* 2018 Feb;286(2):486–498. doi: 10.1148/radiol.2017170550. Epub 2017 Sep 11. [PubMed: 28892458]
14. Schwimmer JB, Middleton MS, Behling C, Newton KP, Awai HI, Paiz MN, et al. Magnetic resonance imaging and liver histology as biomarkers of hepatic steatosis in children with nonalcoholic fatty liver disease. *Hepatology.* 2015 Jun;61(6):1887–95. doi: 10.1002/hep.27666. Epub 2015 Feb 5. [PubMed: 25529941]
15. Caussy C, Reeder SB, Sirlin CB, Loomba R. Non-invasive, quantitative assessment of liver fat by MRI-PDFF as an endpoint in NASH trials. *Hepatology.* 2018;68:763–772 [PubMed: 29356032]
16. Loomba R MRI-Proton Density Fat Fraction Treatment Response Criteria in Nonalcoholic Steatohepatitis. *Hepatology.* 2021 Mar;73(3):881–883. doi: 10.1002/hep.31624. [PubMed: 33179266]

17. Blondiaux E, Chougar L, Gelot A, Valence S, Audureau E, Ducou le Pointe H, et al. Developmental patterns of fetal fat and corresponding signal on T1-weighted magnetic resonance imaging. *Pediatr Radiol*. 2018 Mar;48(3):317–324. doi: 10.1007/s00247-017-4038-z. Epub 2017 Dec 26. [PubMed: 29279948]
18. Victoria T, Jaramillo D, Roberts TP, Zarnow D, Johnson AM, Delgado J, et al. Fetal magnetic resonance imaging: jumping from 1.5 to 3 tesla (preliminary experience). *Pediatr Radiol*. 2014 Apr;44(4):376–86; quiz 373–5. doi: 10.1007/s00247-013-2857-0. Epub 2014 Mar 27. [PubMed: 24671739]
19. Armstrong T, Liu D, Martin T, Masamed R, Janzen C, Wong C, et al. 3D R2\* mapping of the placenta during early gestation using free-breathing multiecho stack-of-radial MRI at 3T. *J Magn Reson Imaging*. 2019 Jan;49(1):291–303. doi: 10.1002/jmri.26203. Epub 2018 Aug 24. [PubMed: 30142239]
20. US Preventive Services Task Force, Davidson KW, Barry MJ, Mangione CM, Cabana M, Caughey AB, et al. Screening for Gestational Diabetes: US Preventive Services Task Force Recommendation Statement. *JAMA*. 2021 Aug 10;326(6):531–538. doi: 10.1001/jama.2021.11922. Erratum in: *JAMA*. 2021 Oct 5;326(13):1331. [PubMed: 34374716]
21. Combs CA, Castillo R, Webb GW, Del Rosario A. Impact of adding abdominal circumference to the definition of fetal growth restriction. *Am J Obstet Gynecol MFM*. 2021 Jul;3(4):100382. doi: 10.1016/j.ajogmf.2021.100382. Epub 2021 Apr 27. [PubMed: 33915330]
22. Zhong X, Nickel MD, Kannengiesser SA, Dale BM, Kiefer B, Bashir MR. Liver fat quantification using a multi-step adaptive fitting approach with multi-echo GRE imaging. *Magn Reson Med*. 2014 Nov;72(5):1353–65. doi: 10.1002/mrm.25054. Epub 2013 Dec 9. [PubMed: 24323332]
23. Mandava S, Keerthivasan MB, Martin DR, Altbach MI, Bilgin A. Radial streak artifact reduction using phased array beamforming. *Magn Reson Med*. 2019 Jun;81(6):3915–3923. doi: 10.1002/mrm.27689. Epub 2019 Feb 12. [PubMed: 30756432]
24. Shih S-F, Wu HH. A Beamforming-Based Coil Combination Method to Reduce Streaking Artifacts and Preserve Phase Fidelity in Radial MRI. *Proceedings of the ISMRM 30th Annual Meeting, 2022*, p1697.
25. Armstrong T, Ly KV, Murthy S, Ghahremani S, Kim GHJ, Calkins KL, et al. Free-breathing quantification of hepatic fat in healthy children and children with nonalcoholic fatty liver disease using a multi-echo 3-D stack-of-radial MRI technique. *Pediatr Radiol*. 2018 Jul;48(7):941–953. doi: 10.1007/s00247-018-4127-7. Epub 2018 May 4. [PubMed: 29728744]
26. Armstrong T, Zhong X, Shih SF, Felker E, Lu DS, Dale BM, et al. Free-breathing 3D stack-of-radial MRI quantification of liver fat and R2\* in adults with fatty liver disease. *Magn Reson Imaging*. 2022 Jan;85:141–152. doi: 10.1016/j.mri.2021.10.016. Epub 2021 Oct 16. [PubMed: 34662702]
27. Story JD, Ghahremani S, Kafali SG, Shih S-F, Kuwahara K, Calkins KL, et al. Using Free-Breathing MRI to Quantify Pancreatic Fat and Investigate Spatial Heterogeneity in Children. *Journal of Magnetic Resonance Imaging 2022*, in press. doi: 10.1002/jmri.28337.
28. Olsen IE, Groveman SA, Lawson ML, Clark RH, Zemel BS. New intrauterine growth curves based on United States data. *Pediatrics*. 2010 Feb;125(2):e214–24. doi: 10.1542/peds.2009-0913. Epub 2010 Jan 25. [PubMed: 20100760]
29. Harris PA, Taylor R, Thielke R, Payne J, Gonzalez N, Conde JG. Research electronic data capture (REDCap)—a metadata-driven methodology and workflow process for providing translational research informatics support. *J Biomed Inform*. 2009 Apr;42(2):377–81. doi: 10.1016/j.jbi.2008.08.010. Epub 2008 Sep 30. [PubMed: 18929686]
30. Berger-Kulemann V, Brugger PC, Reisseger M, Klein K, Hachemian N, Koelblinger C, et al. Quantification of the subcutaneous fat layer with MRI in fetuses of healthy mothers with no underlying metabolic disease vs. fetuses of diabetic and obese mothers. *J Perinat Med*. 2011 Nov 25;40(2):179–84. doi: 10.1515/JPM.2011.122. [PubMed: 22117112]
31. Giza SA, Olmstead C, McCooye DA, Miller MR, Penava DA, Eastabrook GD, et al. Measuring fetal adipose tissue using 3D water-fat magnetic resonance imaging: a feasibility study. *J Matern Fetal Neonatal Med*. 2020 Mar;33(5):831–837. doi: 10.1080/14767058.2018.1506438. Epub 2018 Sep 6. [PubMed: 30189758]

32. Anblagan D, Deshpande R, Jones NW, Costigan C, Bugg G, Raine-Fenning N, et al. Measurement of fetal fat in utero in normal and diabetic pregnancies using magnetic resonance imaging. *Ultrasound Obstet Gynecol.* 2013 Sep;42(3):335–40. doi: 10.1002/uog.12382. [PubMed: 23288811]
33. Kö ü N, Kö ü A. Can fetal abdominal visceral adipose tissue and subcutaneous fat thickness be used for correct estimation of fetal weight? A preliminary study. *J Obstet Gynaecol.* 2019 Jul;39(5):594–600. doi: 10.1080/01443615.2018.1530971. Epub 2019 Apr 22. [PubMed: 31010342]
34. US Preventive Services Task Force, Davidson KW, Barry MJ, Mangione CM, Cabana M, Caughey AB, et al. Behavioral Counseling Interventions for Healthy Weight and Weight Gain in Pregnancy: US Preventive Services Task Force Recommendation Statement. *JAMA.* 2021 May 25;325(20):2087–2093. doi: 10.1001/jama.2021.6949. [PubMed: 34032823]
35. Plows JF, Stanley JL, Baker PN, Reynolds CM, Vickers MH. The Pathophysiology of Gestational Diabetes Mellitus. *Int J Mol Sci.* 2018 Oct 26;19(11):3342. doi: 10.3390/ijms19113342. [PubMed: 30373146]
36. Bader J, Carson M, Enos R, Velazquez K, Sougiannis A, Singh U, et al. High-fat diet-fed ovariectomized mice are susceptible to accelerated subcutaneous tumor growth potentially through adipose tissue inflammation, local insulin-like growth factor release, and tumor associated macrophages. *Oncotarget.* 2020 Dec 8;11(49):4554–4569. doi: 10.18632/oncotarget.27832. [PubMed: 33346251]
37. Zhou Y, Zhao R, Lyu Y, Shi H, Ye W, Tan Y, et al. Serum and Amniotic Fluid Metabolic Profile Changes in Response to Gestational Diabetes Mellitus and the Association with Maternal-Fetal Outcomes. *Nutrients.* 2021 Oct 18;13(10):3644. doi: 10.3390/nu13103644. [PubMed: 34684645]
38. Tan K, Tint MT, Michael N, Yap F, Chong YS, Tan KH, et al. Determinants of cord blood adipokines and association with neonatal abdominal adipose tissue distribution. *Int J Obes (Lond).* 2022 Mar;46(3):637–645. doi: 10.1038/s41366-021-00975-3. Epub 2021 Dec 4. [PubMed: 34864815]
39. Skinner J, O'Donoghue K, Gardeil F, Greene R, Turner MJ. Is fetal abdominal subcutaneous fat comparable with established indices of growth restriction? *J Obstet Gynaecol.* 2001 Sep;21(5):439–42. doi: 10.1080/01443610120071947. [PubMed: 12521793]
40. Brown LD, Hay WW Jr. Impact of placental insufficiency on fetal skeletal muscle growth. *Mol Cell Endocrinol.* 2016 Nov 5;435:69–77. doi: 10.1016/j.mce.2016.03.017. Epub 2016 Mar 16. [PubMed: 26994511]
41. de Fluiter KS, van Beijsterveldt IALP, Breij LM, Acton D, Hokken-Koelega ACS. Association Between Fat Mass in Early Life and Later Fat Mass Trajectories. *JAMA Pediatr.* 2020 Dec 1;174(12):1141–1148. doi: 10.1001/jamapediatrics.2020.2673. [PubMed: 32804197]
42. Ong YY, Sadananthan SA, Aris IM, Tint MT, Yuan WL, Huang JY, et al. Mismatch between poor fetal growth and rapid postnatal weight gain in the first 2 years of life is associated with higher blood pressure and insulin resistance without increased adiposity in childhood: the GUSTO cohort study. *Int J Epidemiol.* 2020 Oct 1;49(5):1591–1603. doi: 10.1093/ije/dyaa143. Erratum in: *Int J Epidemiol.* 2021 May 17;50(2):702. [PubMed: 32851407]
43. Rolland-Cachera MF, Péneau S. Growth trajectories associated with adult obesity. *World Rev Nutr Diet.* 2013;106:127–34. doi: 10.1159/000342564. Epub 2013 Feb 11. [PubMed: 23428691]
44. Sinclair KJ, Friesen-Waldner LJ, McCurdy CM, Wiens CN, Wade TP, de Vrijer B, et al. Quantification of fetal organ volume and fat deposition following in utero exposure to maternal Western Diet using MRI. *PLoS One.* 2018 Feb 15;13(2):e0192900. doi: 10.1371/journal.pone.0192900. [PubMed: 29447203]
45. Huang SW, Ou YC, Tang KS, Yu HR, Huang LT, Tain YL, et al. Metformin ameliorates maternal high-fat diet-induced maternal dysbiosis and fetal liver apoptosis. *Lipids Health Dis.* 2021 Sep 8;20(1):100. doi: 10.1186/s12944-021-01521-w. [PubMed: 34496884]
46. Wang YW, Yu HR, Tiao MM, Tain YL, Lin IC, Sheen JM, et al. Maternal Obesity Related to High Fat Diet Induces Placenta Remodeling and Gut Microbiome Shaping That Are Responsible for Fetal Liver Lipid Dysmetabolism. *Front Nutr.* 2021 Dec 15;8:736944. doi: 10.3389/fnut.2021.736944. [PubMed: 34977107]



47. Chang GQ, Gaysinskaya V, Karatayev O, Leibowitz SF. Maternal high-fat diet and fetal programming: increased proliferation of hypothalamic peptide-producing neurons that increase risk for overeating and obesity. *J Neurosci*. 2008 Nov 12;28(46):12107–19. doi: 10.1523/JNEUROSCI.2642-08.2008. [PubMed: 19005075]
48. Kislal S, Shook LL, Edlow AG. Perinatal exposure to maternal obesity: Lasting cardiometabolic impact on offspring. *Prenat Diagn*. 2020 Aug;40(9):1109–1125. doi: 10.1002/pd.5784. Epub 2020 Aug 5. [PubMed: 32643194]
49. Lindberger E, Wikström AK, Bergman E, Eurenus K, Mulic-Lutvica A, Sundström Poromaa I, et al. Association of maternal central adiposity measured by ultrasound in early mid pregnancy with infant birth size. *Sci Rep*. 2020 Nov 12;10(1):19702. doi: 10.1038/s41598-020-76741-8. [PubMed: 33184361]
50. Jarvie EM, Stewart FM, Ramsay JE, Brown EA, Meyer BJ, Olivecrona G, et al. Maternal Adipose Tissue Expansion, A Missing Link in the Prediction of Birth Weight Centile. *J Clin Endocrinol Metab*. 2020 Mar 1;105(3):dgz248. doi: 10.1210/clinem/dgz248. [PubMed: 31832635]
51. Paula VG, Sinzato YK, de Moraes-Souza RQ, Soares TS, Souza FQG, Karki B, et al. Metabolic changes in female rats exposed to intrauterine hyperglycemia and postweaning consumption of high-fat diet†. *Biol Reprod*. 2022 Jan 13;106(1):200–212. doi: 10.1093/biolre/ioab195. [PubMed: 34668971]
52. Haghiaç M, Basu S, Presley L, Serre D, Catalano PM, Hauguel-de Mouzon S. Patterns of adiponectin expression in term pregnancy: impact of obesity. *J Clin Endocrinol Metab*. 2014 Sep;99(9):3427–34. doi: 10.1210/jc.2013-4074. Epub 2014 May 5. [PubMed: 24796925]
53. Ikenoue S, Kasuga Y, Endo T, Tanaka M, Ochiai D. Newer Insights Into Fetal Growth and Body Composition. *Front Endocrinol (Lausanne)*. 2021 Jul 22;12:708767. doi: 10.3389/fendo.2021.708767. [PubMed: 34367074]
54. Catalano PM, Thomas A, Huston-Presley L, Amini SB. Increased fetal adiposity: a very sensitive marker of abnormal in utero development. *Am J Obstet Gynecol*. 2003 Dec;189(6):1698–704. doi: 10.1016/s0002-9378(03)00828-7. [PubMed: 14710101]
55. Brumbaugh DE, Tearse P, Cree-Green M, Fenton LZ, Brown M, Scherzinger A, et al. Intrahepatic fat is increased in the neonatal offspring of obese women with gestational diabetes. *J Pediatr*. 2013 May;162(5):930–6.e1. doi: 10.1016/j.jpeds.2012.11.017. Epub 2012 Dec 20. [PubMed: 23260099]
56. Shulman M, Cho E, Aasi B, Cheng J, Nithiyantham S, Waddell N, et al. Quantitative analysis of fetal magnetic resonance phantoms and recommendations for an anthropomorphic motion phantom. *MAGMA*. 2020 Apr;33(2):257–272. doi: 10.1007/s10334-019-00775-x. Epub 2019 Sep 5. [PubMed: 31487004]
57. Satkunasingham J, Nik HH, Fischer S, Menezes R, Selzner N, Cattral M, et al. Can negligible hepatic steatosis determined by magnetic resonance imaging-proton density fat fraction obviate the need for liver biopsy in potential liver donors? *Liver Transpl*. 2018 Apr;24(4):470–477. doi: 10.1002/lt.24965. Epub 2018 Mar 6. [PubMed: 29080242]



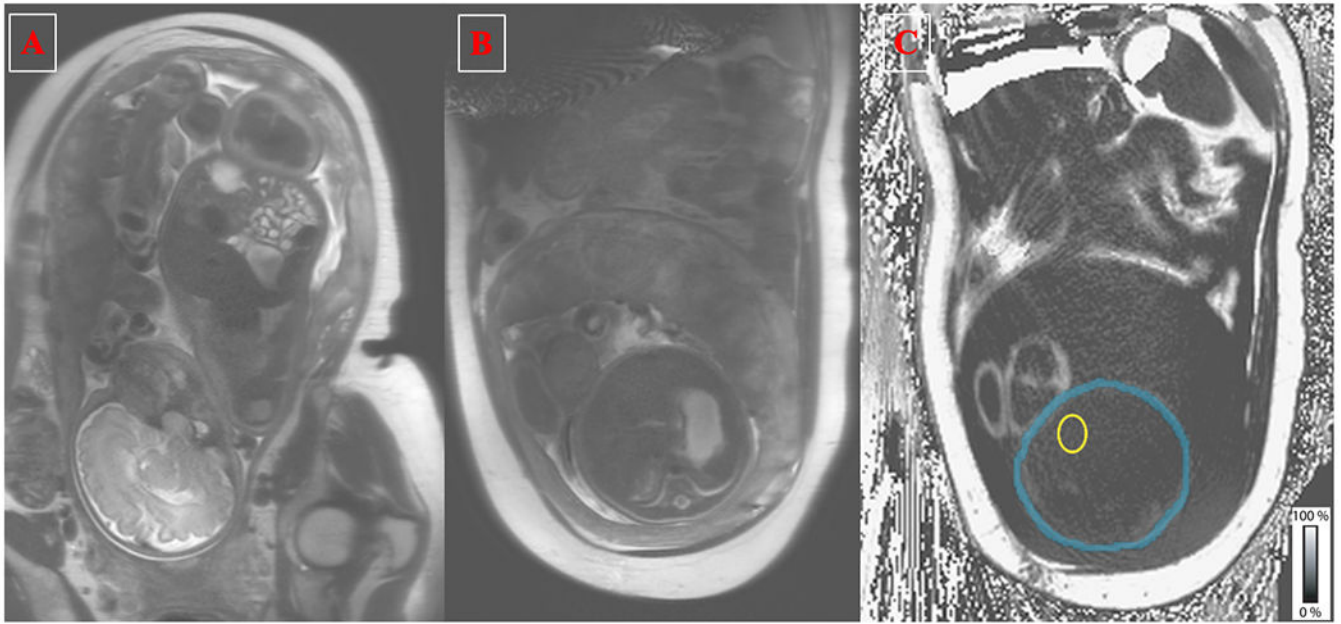


**Figure 1.** Fetal body composition measurements on MRI. This figure shows a fetus whose mother had gestational diabetes. **A.** Image from a sagittal T<sub>2</sub>-weighted (T<sub>2</sub>W) half-Fourier acquisition single-shot turbo spin-echo (HASTE) sequence. **B.** Image from an axial T<sub>2</sub>W HASTE sequence. **C.** Proton-density fat fraction (PDFF) map from a free-breathing 3-D stack-of-radial gradient echo sequence. As shown by the grayscale bar for PDFF values (0-100%), white pixels have high fat content and dark pixels have low fat content. The images in B and C are matched at the level of the lower liver. The blue annotation represents fetal subcutaneous fat. The yellow oval is a 3-cm<sup>2</sup> region of interest used to measure fetal hepatic PDFF.

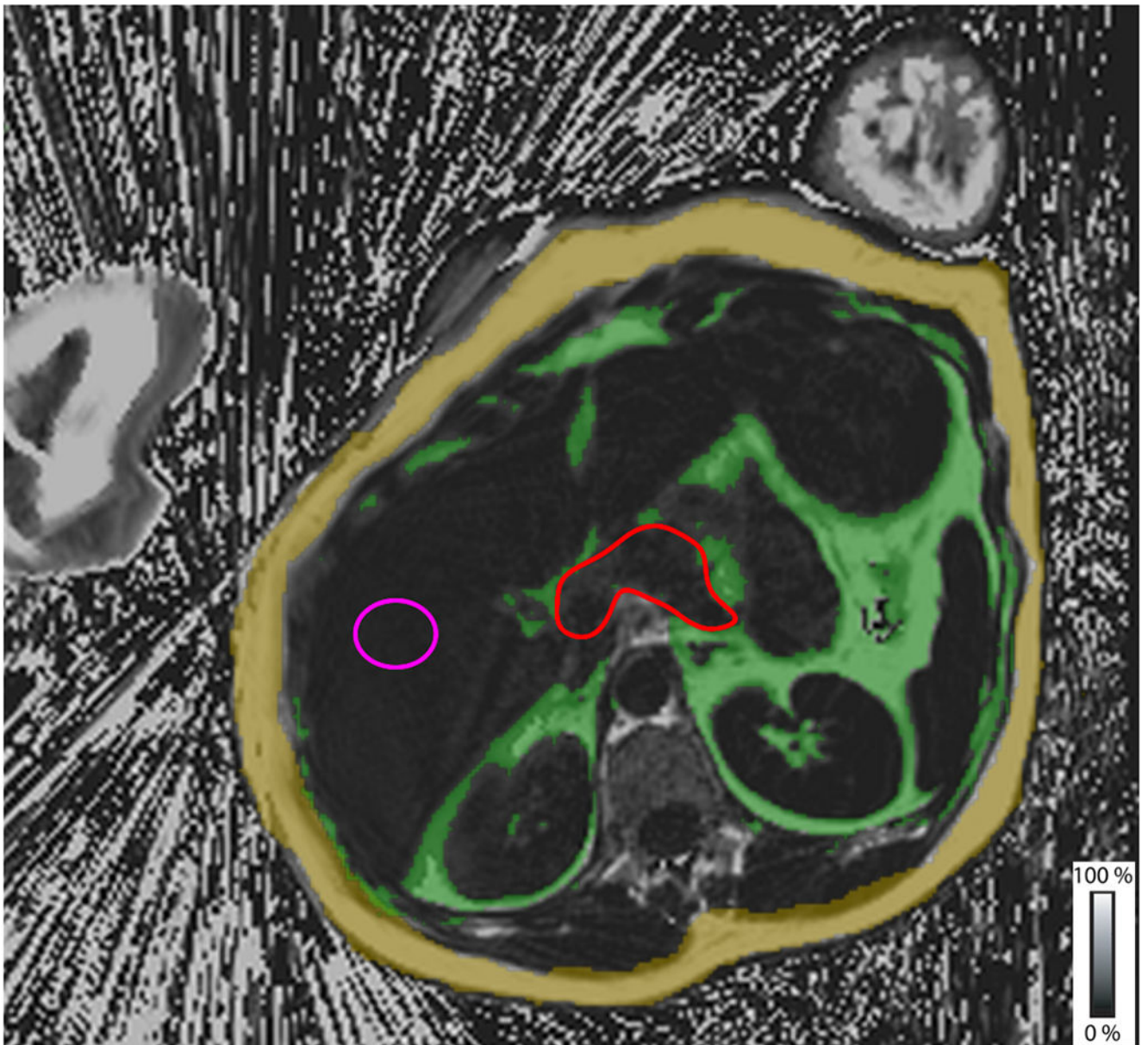


**Figure 2.** Maternal body composition measurements on a proton-density fat fraction (PDFF) map from free-breathing MRI. As shown by the grayscale bar for PDFF values (0-100%), white pixels have high fat content and dark pixels have low fat content. The yellow annotation represents subcutaneous adipose tissue. The green region represents visceral adipose tissue. The magenta 5-cm<sup>2</sup> region of interest was used to measure maternal liver PDFF. The red contour outlines the maternal pancreas.

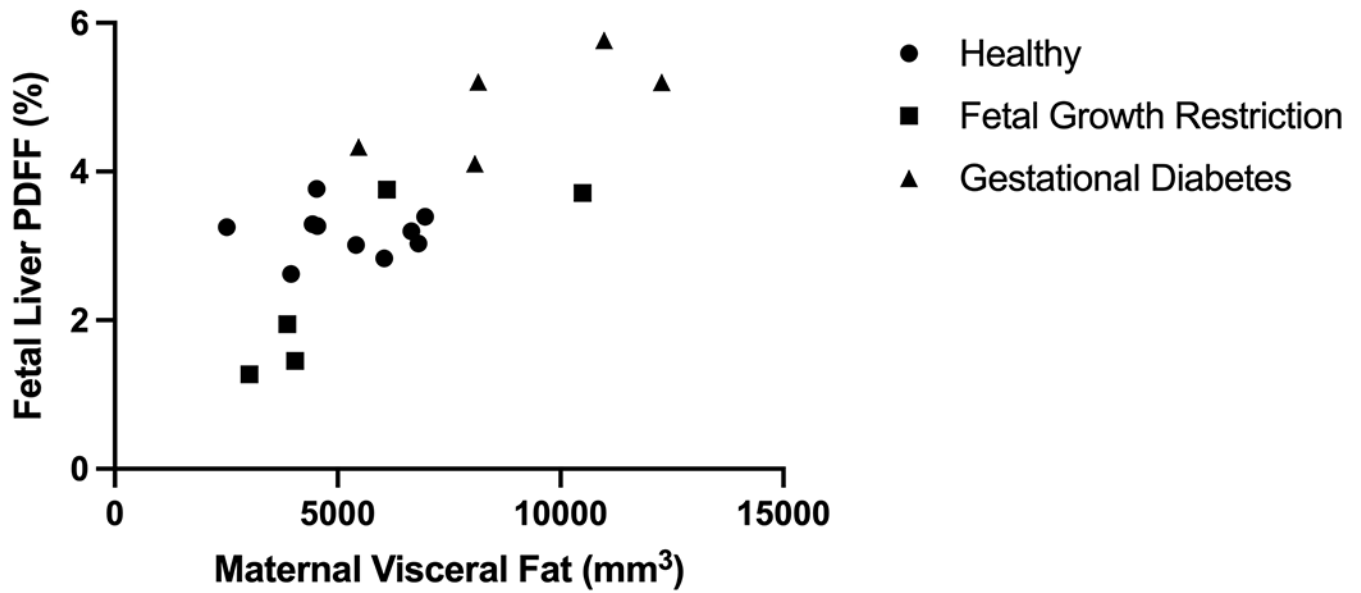


**Figure 3.** Relationship between fetal hepatic proton-density fat fraction (PDFF) (%) and maternal visceral fat volume (mm<sup>3</sup>) utilizing Spearman correlation. Circles represent the healthy pregnancies. Squares represent pregnancies with fetal growth restriction. Triangles represent pregnancies with gestational diabetes.

**Table 1.**

Characteristics of the maternal-fetus dyads. Categorical values are represented as percent (n).

	Healthy Pregnancies (N=10)	Gestational Diabetes Pregnancies (N=5)	Fetal Growth Restriction Pregnancies (N=5)	p-value
Maternal age (years)	34.5 (29.8, 38)	33 (30.5, 36.5)	35 (27.5, 36)	0.80
Pre-pregnancy BMI (kg/m <sup>2</sup> )	23.9 (21.9, 26.2)	31 (27.6, 32.5)	22.7 (20.6, 33.3)	0.10
Weight gain in pregnancy (kg)	14.1 (14.1, 16.9) <sup>*</sup>	10.9 (5.1, 12.1)	13.4 (8.5, 15.9)	0.03
Race	30 (3) Asian 70 (7) White	100 (10) White	40 (4) Asian 60 (6) White	0.30
Hispanic Ethnicity	20 (2)	80 (8)	20 (2)	0.08
Glucose tolerance test at 1 hour (mg/dL)	87 (67, 112) <sup>*</sup>	182 (157, 191)	131 (102, 146)	0.005
Gestational age at time of MRI (weeks)	32.7 (32.3, 34.5)	35.3 (32.9, 35.7)	33.4 (31.7, 34)	0.27
Gestational age at delivery (weeks)	39.4 (37.8, 41.1)	38.1 (37.5, 39.8)	38.4 (35.3, 39.7)	0.31
Vaginal delivery	90 (9)	100 (10)	60 (6)	0.57
NICU admission	0 (0)	0 (0)	80 (4)	0.04
Birth weight (g)	3322 (2850, 3548)	3085 (2830, 3499)	2100 (1524, 3175)	0.13
Birth weight z-score	0.09 (-0.7, 0.2)	0.2 (-0.8, 0.5)	-1.8 (-2.3, -0.5)	0.05
Birth length (cm)	51 (49.3, 53.7)	50.5 (47.8, 50.8)	45.0 (40.1, 50.5)	0.17
Birth length z-score	0.4 (-0.2, 0.7)	0.2 (-0.9, 0.5)	-1.2 (-2.3, 0.04)	0.07
Birth head circumference z-score	-0.4 (-0.9, 0.4)	1.4 (-2, 1.6)	-1.2 (-2.4, -0.4)	0.23
Birth BMI z-score	-0.85 (-1.25, 0.01)	-0.08 (-0.49, 0.38)	-1.21 (-1.7, 0.1)	0.24

<sup>\*</sup>p<0.05 compared to pregnancies with gestational diabetes mellitus.

<sup>+</sup>p=0.10 compared to pregnancies with gestational diabetes mellitus.

BMI: body mass index. NICU: neonatal intensive care unit.

**Table 2.**

Fetal and maternal body composition parameters. Continuous variables represented as median (IQR).

	Healthy Pregnancies (N=10)	Gestational Diabetes Pregnancies (N=5)	Fetal Growth Restriction Pregnancies (N=5)	p-value
<b>Fetal subcutaneous adipose tissue volume (mm<sup>3</sup>)</b>	241 (232, 255) <sup>‡</sup>	280 (261, 295)	220 (205, 235) <sup>*</sup>	0.003
<b>Fetal liver PDFF (%)</b>	3.2 (3.0, 3.3) <sup>*</sup>	5.2 (4.2, 5.5)	1.9 (1.4, 3.7) <sup>*</sup>	0.004
<b>Maternal subcutaneous adipose tissue volume (mm<sup>3</sup>)</b>	157,319 (126,300, 200,028)	216,264 (161,461, 325,975)	159,197 (84,024, 339,707)	0.40
<b>Maternal visceral adipose tissue volume (mm<sup>3</sup>)</b>	97,593 (78,014, 121,081) <sup>*</sup>	169,626 (137,736, 227,035)	96,787 (82,327, 184,784)	0.03
<b>Maternal liver PDFF (%)</b>	2.1 (1.8, 2.8)	3.2 (2.1, 3.8)	2.2 (1.1, 5.0)	0.43
<b>Maternal pancreatic PDFF (%)</b>	6.6 (5.8, 7.4)	10.0 (7.6, 13.0)	5.5 (4.1, 7.2) <sup>*</sup>	0.03

\* p<0.05 compared to pregnancies with gestational diabetes mellitus.

‡ p=0.10 compared to pregnancies with gestational diabetes mellitus.

PDFF: proton density fat fraction.